

# Voltage Reflex and Equalization Charger for Series-connected Batteries

Cheng-Tao Tsai\* and Jia-Wei Lin

Department of Electrical Engineering, National Chin-Yi University of Technology,  
No. 57, Sec. 2, Zhongshan Rd., Taiping Dist. Taichung City 41170, Taiwan

(Received May 27, 2025; accepted January 5, 2026)

**Keywords:** series-connected, lithium iron phosphate, real-time monitoring

In this paper, a charger with the functions of voltage reflex and equalization is proposed. The proposed charger for series-connected lithium iron phosphate (LFP) batteries has the following advantages: (1) a voltage reflex circuit is used to obtain a fast charging response and high charging efficiency, and (2) a voltage equalization circuit is used to obtain a voltage balance and extend the lifecycle. Additionally, to achieve the protective functions for charging voltage and current, the proposed charger incorporates a real-time monitoring circuit with LED indicators. Finally, to verify its feasibility, we built a prototype of the voltage reflex and equalization charger. The experimental results are presented to demonstrate the performance of the voltage reflex and equalization charger.

## 1. Introduction

Technological progress and rapid development promote the convenience and raise the comfort of human beings, which has made people highly dependent on electronic products. Energy acquisition will be an important issue in the future.<sup>(1,2)</sup> Batteries are one of the power sources for electronic products. Rechargeable batteries include lead-acid batteries, nickel–cadmium batteries, nickel–metal hydride batteries, and lithium iron phosphate (LFP) batteries. Among them, LFP batteries have the advantages of best lifecycle, high energy density, and no pollution.<sup>(3–5)</sup> Currently, many companies have actively invested in the research, development, and manufacture of LFP batteries. The voltage of a single LFP battery equals that of three nickel–cadmium batteries connected in series. Therefore, the probability of damage can be reduced when charging series-connected LFP batteries.<sup>(6–8)</sup>

The traditional charging methods of LFP batteries are series charging and parallel charging. In many practical applications, the LFP batteries connected in series can provide higher voltages. The differences between charging and discharging rates result in voltage imbalances in series-connected LFP batteries.<sup>(9–12)</sup> Therefore, the charging techniques of the series-connected LFP batteries are a timely research topic.<sup>(13–15)</sup> To overcome voltage imbalances in series-connected

---

\*Corresponding author: e-mail: [cttsai@ncut.edu.tw](mailto:cttsai@ncut.edu.tw)  
<https://doi.org/10.18494/SAM5754>

LFP batteries, a charger incorporated with a voltage reflex and a voltage equalization circuit is proposed, as shown in Fig. 1. The proposed charger for the applications of the series-connected LFP batteries has the advantages of achieving a fast charging response, a high charging efficiency as well as voltage balance, and an extended lifecycle. The operational principles of the voltage reflex and equalization charger are described in Sect. 2. The control processes of the voltage reflex and equalization charger are described in Sect. 3. The experimental results to verify the feasibility of the voltage reflex and equalization charger are shown in Sect. 4. Finally, conclusions are given in Sect. 5.

## 2. Operational Principles of Voltage Reflex and Equalization Charger

The operational principles of the voltage reflex and equalization charger can be divided into four modes under a charging cycle, as shown in Fig. 2. For the convenience of illustration and analysis, the voltage reflex and equalization charger is divided into a voltage reflex circuit and a voltage equalization circuit, as shown in Fig 1.

### 2.1 Operational principles of voltage reflex circuit

The operational principles of the voltage reflex circuit are divided into three modes. Figure 3 shows the equivalent circuits of the three modes.

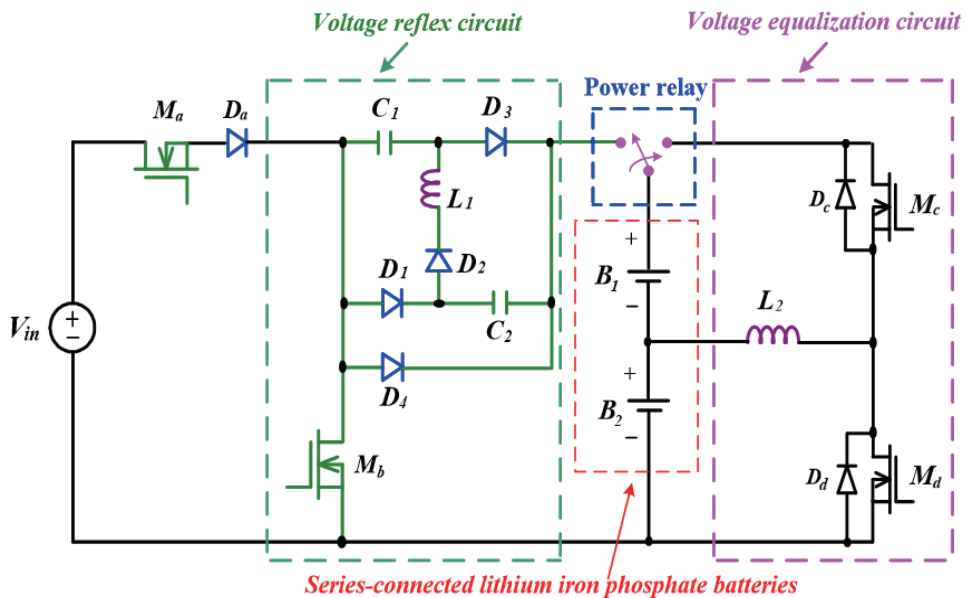


Fig. 1. (Color online) Voltage reflex and equalization charger.

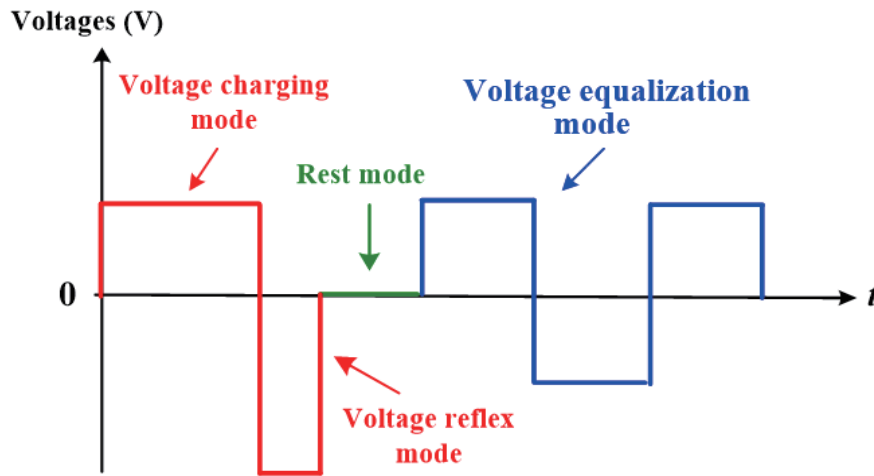


Fig. 2. (Color online) Operational modes of voltage reflex and equalization in one charging cycle.

### Mode 1: voltage charging mode

The switch  $M_a$  is turned on and  $M_b$  is turned off at the voltage charging mode of the series-connected LFP batteries. The diodes  $D_1$  and  $D_2$  are turned on and  $D_4$  is turned off. The voltages of the capacitors  $C_1$  and  $C_2$  will be discharged. When the voltages of  $C_1$  and  $C_2$  drop to zero,  $D_1$  and  $D_2$  are turned off and  $D_4$  is turned on. During this interval, the series-connected LFP batteries are charged. The equivalent circuit of the operational mode 1 is shown in Figs. 3(a) and 3(b).

### Mode 2: voltage reflex mode

The switch  $M_a$  is turned off and  $M_b$  is turned on at the voltage charging mode of the series-connected LFP batteries. The diode  $D_2$  is turned on and  $D_4$  is turned off. During this interval, the voltages of the series-connected LFP batteries flowing through the reflex loop are charged. The equivalent circuit of operational mode 2 is shown in Fig. 3(c).

### Mode 3: rest mode

After voltage charging and reflex modes have been completed in the series-connected LFP batteries, they are operated in the rest mode. The equivalent circuit of operational mode 3 is shown in Fig. 3(d). The series-connected LFP batteries are completed in a voltage charging and reflex period.

## 2.2 Operational principles of voltage equalization circuit

The operational principles of the voltage equalization circuit are divided into six modes. Figure 4 shows the equivalent circuits of the six modes.

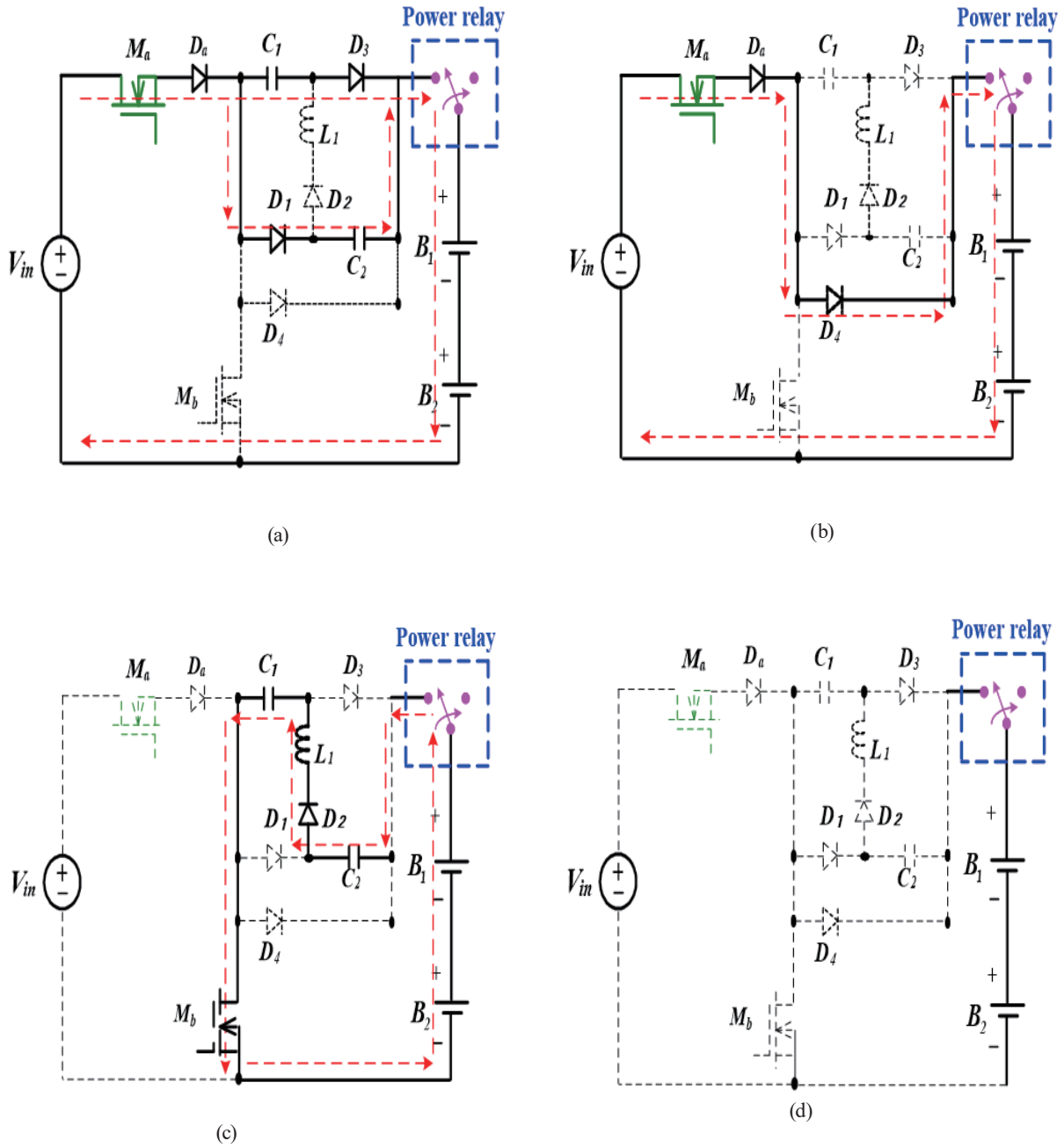


Fig. 3. (Color online) Equivalent circuits of the three modes.

**Mode 1: discharging mode of LFP battery  $B_1$**

While the switch  $M_c$  is turned on and  $M_d$  is turned off, the LFP battery  $B_1$  is discharging. The discharging loop flows through the path  $B_1 \rightarrow M_c \rightarrow L_2$ . The equivalent circuit of mode 1 is shown in Fig. 4(a).

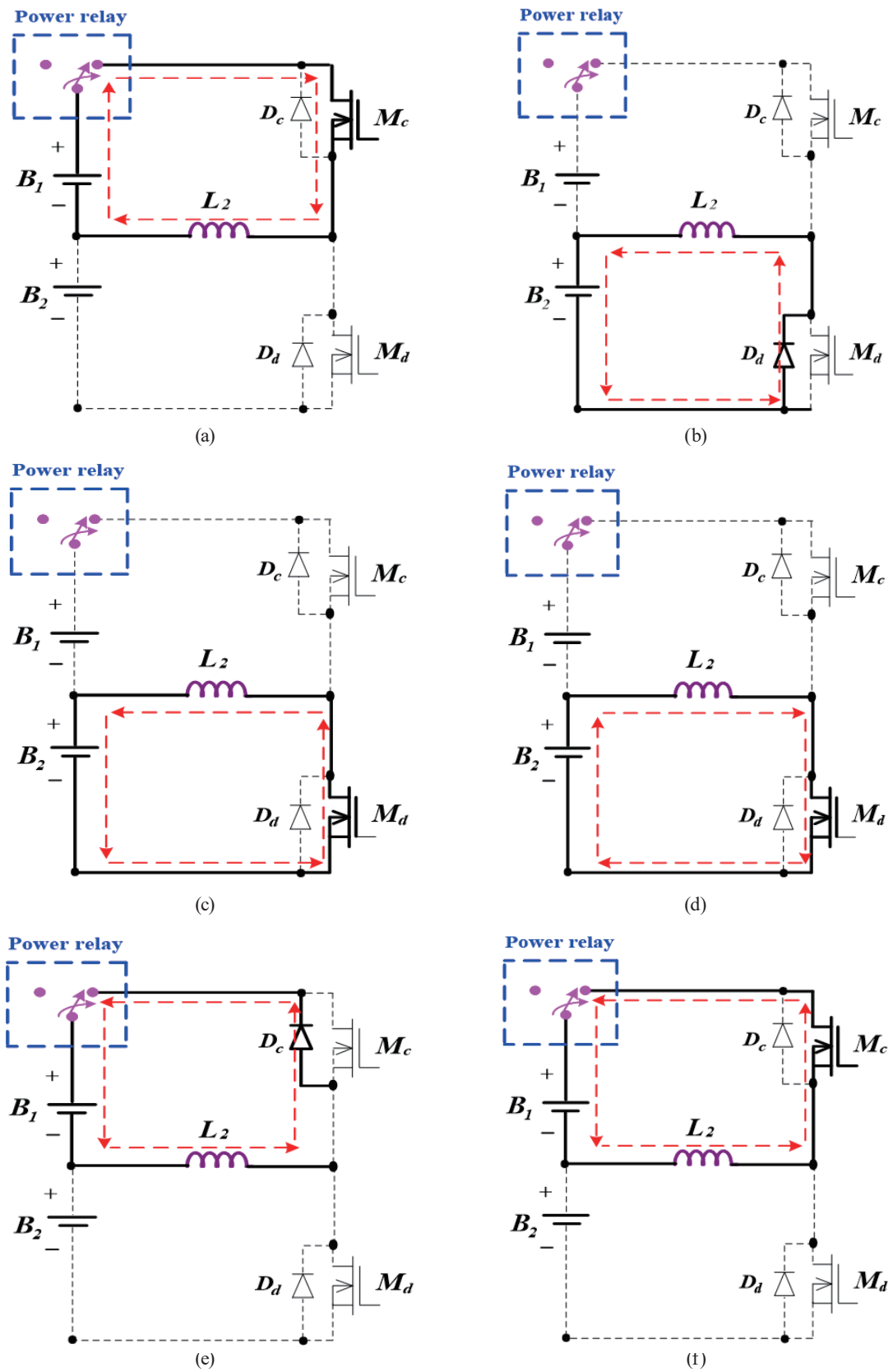


Fig. 4. (Color online) Equivalent circuits of the six modes.

### Mode 2: charging mode of LFP battery $B_2$

While the switches  $M_c$  and  $M_d$  are turned off, the LFP battery  $B_1$  stops discharging and  $B_2$  begins charging. The charging loop flows through the path  $L_2 \rightarrow B_2 \rightarrow D_d$ . While  $M_d$  is turned on, the charging loop flows through the path  $L_2 \rightarrow B_2 \rightarrow M_d$ . The equivalent circuit of mode 2 is shown in Figs. 4(b) and 4(c).

### Mode 3: discharging mode of LFP battery $B_2$

When the energy of the inductor  $L_2$  drops to zero, the LFP battery  $B_2$  starts discharging. The discharging loop flows through the path  $B_2 \rightarrow L_2 \rightarrow M_d$ . The equivalent circuit of mode 3 is shown in Fig. 4(d).

### Mode 4: charging mode of LFP battery $B_1$

While switches  $M_c$  and  $M_d$  are turned off, the LFP battery  $B_1$  is charging and  $B_2$  stops discharging. The charging loop flows through the path  $L_2 \rightarrow D_c \rightarrow B_1$ . While  $M_c$  is turned on, the charging loop flows through the path  $L_2 \rightarrow M_c \rightarrow B_1$ . The equivalent circuit of mode 4 is shown in Figs. 4(e) and 4(f). The voltage equalization of the series-connected LFP batteries is completed in the procedure of charging and discharging.

## 3. Control Mechanism of Voltage Reflex and Equalization Charger

The voltage reflex and equalization charger uses a TMS320F240 microcontroller to implement the optimal control mechanism of the series-connected LFP batteries. The control flowchart and conceptual diagram are shown in Figs. 5 and 6. The voltage and current signals of the LFP batteries are sensed and sent to the TMS320F240 microcontroller. By comparing these

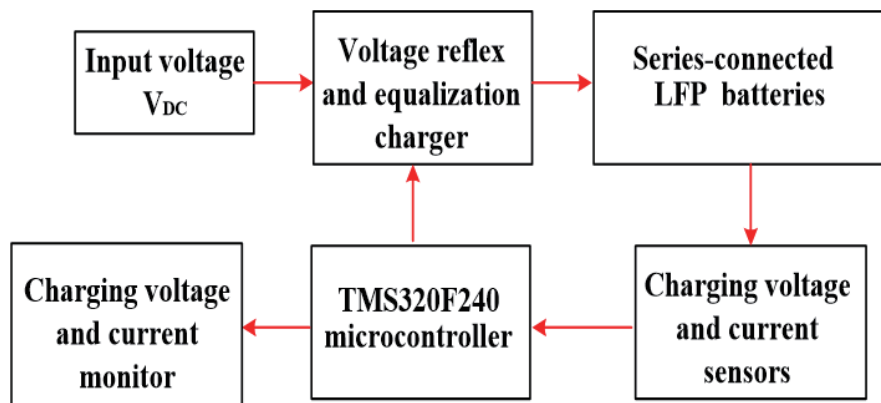


Fig. 5. (Color online) Control flowchart of voltage reflex and equalization charger.

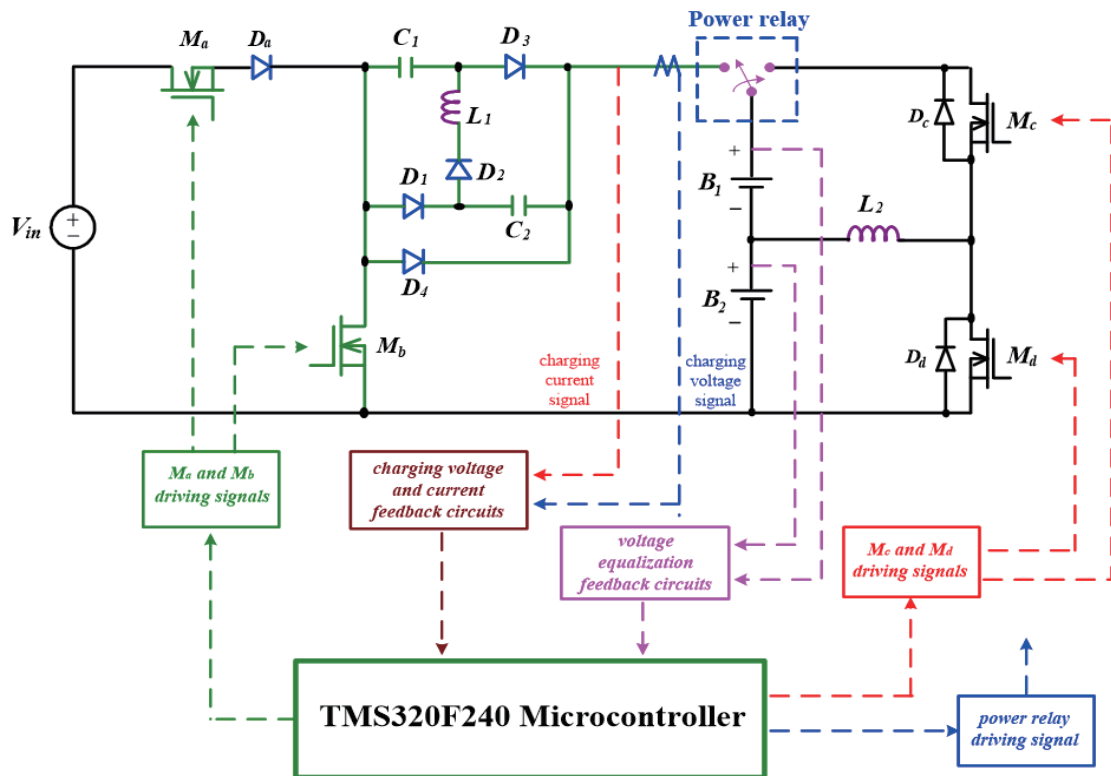


Fig. 6. (Color online) Conceptual diagram of voltage reflex and equalization charger.

signals, the TMS320F240 microcontroller will generate suitable driving signals of switches  $M_a$ ,  $M_b$ ,  $M_c$ , and  $M_d$ . Therefore, the optimal control mechanism can be achieved by the voltage reflex and equalization of the series-connected LFP batteries.

#### 4. Experimental Results

To verify the performance of the proposed charger, a prototype voltage reflex and equalization charger is built. Its specifications are listed as follows.

- input voltage of voltage reflex and equalization charger:  $V_{in} = 52 \text{ V}_{\text{DC}}$ ,
- full charging voltage of series-connected LFP batteries:  $V_{bat} = 50 \text{ V}_{\text{DC}}$ ,

Figure 7 shows driving signals of switches  $M_a$ ,  $M_b$ ,  $M_c$ , and  $M_d$ . The charging voltage and current signals are delivered via the feedback circuits to the TMS320F240 microcontroller to obtain all driving signals of the switches. Figure 8 shows the charging voltage and current waveforms of the series-connected LFP batteries. From the measurement results in Fig. 8, it can

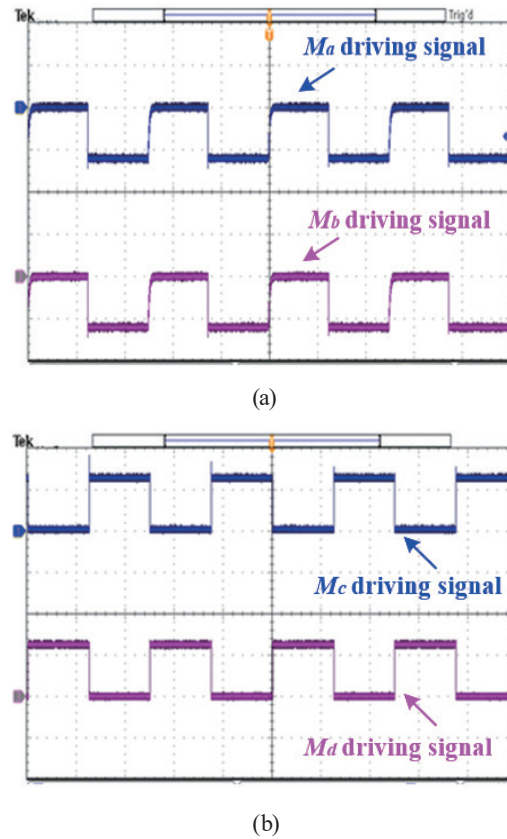


Fig. 7. (Color online) Measured driving signals of switches: (a)  $M_a$  and  $M_b$ , (b)  $M_c$  and  $M_d$ .

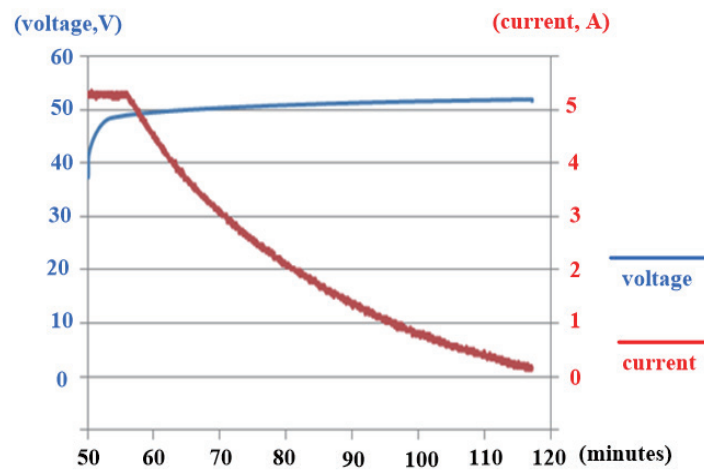


Fig. 8. (Color online) Measured charging voltage and current waveforms of series-connected LFP batteries.

be seen that the series-connected LFP batteries can be charged quickly in a short time via the voltage reflex and equalization charger. Figure 9 shows a test voltage reflex and equalization charger used to verify its feasibility.

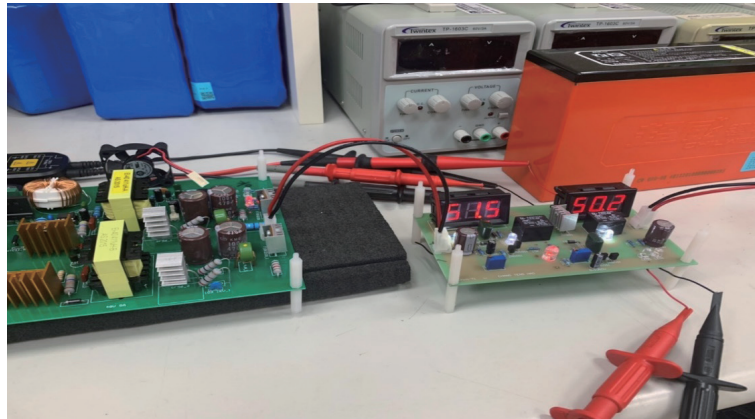


Fig. 9. (Color online) Test voltage reflex and equalization charger.

## 5. Conclusions

A voltage reflex and equalization charger was built and implemented. It consists of a voltage reflex circuit, a voltage equalization circuit, and a TMS320F240 microcontroller to implement the fast charging of series-connected LFP batteries. Experimental results have verified that the voltage reflex and equalization charger is suitable for application to series-connected LFP batteries.

## Acknowledgments

This work was supported by National Chin-Yi University of Technology, Taiwan.

## Author Contributions

Cheng-Tao Tsai designed the circuit and wrote the paper. Jia-Wei Lin analyzed the experimental results.

## Conflicts of Interests

The authors declare no conflicts of interest.

## References

- 1 S. M. Chen, T. J. Liang, L. S. Yang, and J. F. Chen: IEEE Trans. Power Electron. **26** (2011) 1146. <https://doi.org/10.1109/TPEL.2010.2090362>
- 2 C. A. Gallo, F. L. Tofoli, and J. A. C. Pinto: IEEE Trans. Power Electron. **25** (2010) 775. <https://doi.org/10.1109/TPEL.2009.2033063>
- 3 S. W. Lee and H. L. Do: IEEE Trans. Power Electron. **32** (2017) 1375. <https://doi.org/10.1109/TPEL.2016.2549029>

- 4 A. A. Tropina, L. Lenarduzzi, S. V. Marasov, and A. P. Kuzmenko: *IEEE Trans. Plasma Sci.* **37** (2009) 2286. <https://doi.org/10.1109/TPS.2009.2029692>
- 5 H. Wang, H. S. H. Chung, and A. Ioinovici: *IEEE Trans. Power Electron.* **27** (2012) 2242. <https://doi.org/10.1109/TPEL.2011.2173588>
- 6 M. Borage, S. Tiwari, and S. Kotaiah: *IEEE Trans. Ind. Electron.* **52** (2005) 1547. <https://doi.org/10.1109/TIE.2005.858729>
- 7 C. Koroneos, T. Spachos, and N. Moussiopoulos: *Renewable Energy* **28** (2003) 295. [https://doi.org/10.1016/S0960-1481\(01\)00125-2](https://doi.org/10.1016/S0960-1481(01)00125-2)
- 8 I. Batarseh: *IEEE Trans. Power Electron.* **9** (1994) 64. <https://doi.org/10.1109/63.285495>
- 9 G. Carrara, S. Gardella, M. Marchesoni, R. Salutari, and G. Sciutto: *IEEE Trans. Power Electron.* **7** (1992) 497. <https://doi.org/10.1109/63.145137>
- 10 W. Hao, J. Gong, X. Zhao, C. S. Yeh, and J. S. Lai: *IEEE Trans. Power Electron.* **34** (2019) 11952. <https://doi.org/10.1109/TPEL.2019.2909426>
- 11 S. Yang, J. Wang, and W. Yang: *IEEE Trans. Power Electron.* **32** (2017) 1885. <https://doi.org/10.1109/TPEL.2016.2560200>
- 12 B. Singh, S. Gairola, B. N. Singh, A. Chandra, and K. Al-Haddad: *IEEE Trans. Power Electron.* **23** (2008) 260. <https://doi.org/10.1109/TPEL.2007.911880>
- 13 R. L. Steigerwald: *IEEE Trans. Power Electron.* **3** (1988) 174. <https://doi.org/10.1109/63.4347>
- 14 W. Hao, J. Gong, X. Zhao, C. S. Yeh, and J. S. Lai: *IEEE Trans. Power Electron.* **34** (2019) 11952. <https://doi.org/10.1109/TPEL.2019.2909426>
- 15 H. P. Park and J. H. Jung: *Ind. Electron.* **64** (2016) 253. <https://doi.org/10.1109/TIE.2016.2599138>